Radiochim. Acta **93**, 65–73 (2005)

Transmutation experiments on ^{129}I, ^{139}La and ^{237}Np using the Nuclotron accelerator

By W. Westmeier[1,7,*], R. Brandt[1], E.-J. Langrock[2], H. Robotham[7], K. Siemon[7], R. Odoj[3], J. Adam[4,8], V. Bradnova[4], V. M. Golovatyuk[4], V. A. Krasnov[4], M. I. Krivopustov[4], V. S. Pronskikh[4], A. N. Sosnin[4], V. M. Tsoupko-Sitnikov[4], N. M. Vladimirova[4], S. R. Hashemi-Nezhad[5] and M. Zamani-Valasiadou[6]

[1] Fachbereich Chemie, Kernchemie, Philipps-Universität, D-35032 Marburg, Germany
[2] Forschungsbüro Langrock, D-02977 Hoyerswerda, Germany
[3] Institut für Sicherheitsforschung und Reaktortechnik, Forschungszentrum Jülich GmbH, D-52425 Jülich, Germany
[4] Joint Institute for Nuclear Research, Dubna, Russian Federation
[5] Department of High Energy Physics, University of Sydney, Sydney, Australia
[6] Physics Department, Aristotle University, Thessaloniki, Greece
[7] Dr. Westmeier GmbH, Möllner Weg 32, D-35085 Ebsdorfergrund, Germany
[8] Nuclear Physics Institute, Řež, Czech Republic

(Received January 21, 2004; accepted in final form July 29, 2004)

Transmutation / Relativistic proton beam / Moderator / Pb *target /* ^{129}I, ^{139}La, ^{237}Np */ Neutron spectra / B-value*

Summary. Transmutation experiments have been carried out using the NUCLOTRON, a new accelerator for relativistic particles. The experiments were carried out in the Veksler and Baldin Laboratory of High Energies of the Joint Institute for Nuclear Research in Dubna, Russian Federation. Earlier experiments using an 8 cm ∅ Pb-target of 20 cm length and surrounded by 6 cm paraffin (GAMMA-2 target) have been continued to study the transmutation of ^{139}La and the highly radiotoxic radwaste nuclides ^{129}I and ^{237}Np using spallation neutrons produced by relativistic protons with energies $0.5\,\text{GeV} \leq E_\text{p} \leq 4.15\,\text{GeV}$. Results of previous experiments were complemented with additional results, thus yielding data systematics with small uncertainties over the probably commercially relevant energy range of $0.5\,\text{GeV} \leq E_\text{p} \leq 1.0\,\text{GeV}$ and also in the scientifically interesting range above 1 GeV. Moreover, neutron density distributions in irradiations with 0.65 GeV, 1 GeV and 3.7 GeV protons were determined on the surface of the paraffin moderator for two energy regimes of slow and intermediate/fast neutrons. A large set of high quality experimental data with small uncertainties has been generated that can serve as benchmark data for modelling purposes.

1. Introduction

The completion of the new accelerator NUCLOTRON [1] at the Veksler and Baldin Laboratory of High Energies (LHE) of the Joint Institute for Nuclear Research (JINR) in Dubna, Russia, is a remarkable achievement in the construction of advanced accelerators for relativistic particles and it opens the door to a broad spectrum of exciting new experiments. The accelerator ring of the NUCLOTRON is operated at the temperature of liquid helium, thus allowing a very efficient use of electrical power to produce relativistic protons and heavy ions of energies up to 6 GeV/nucleon. In the initial phase of the operation only relativistic protons with energies up to about 5 GeV were used to study transmutation of long-lived radioactive waste. Highly radioactive waste is being accumulated through the continued operation of commercial nuclear power plants and other nuclear facilities. Large quantities of such waste constitute a very serious problem for mankind both from a commercial as well as from an ecological and safety point of view. A decade ago several teams suggested the development of subcritical nuclear assemblies [2, 3] which are ignited and upheld by relativistic particles for the transmutation of long-lived radioactive waste. Typical examples of long-lived and highly radiotoxic nuclides that can be transmuted into short-lived or stable nuclei are ^{237}Np and ^{129}I. An essential technical step for transmutation is the production of large amounts of neutrons through spallation reactions induced by relativistic protons in heavy target materials. The energy spectrum of spallation neutrons extends up to a few hundred MeV. The exact shape of the neutron energy spectrum depends on a wide range of parameters, such as the position within the target assembly, the target composition and others. Studies of these and associated problems have also been carried out during recent years [4–7] – among others – at the Laboratory of High Energies (LHE), Dubna and in CERN, Geneva for proton energies above 0.5 GeV.

The present work is a continuation of these investigations in the LHE in Dubna. A successful feasibility study about using the new accelerator NUCLOTRON for such investigations is reported in [8]. The present paper focuses on the development of precise and well-controlled irradiation conditions for ongoing transmutation investigations. Technical details for accurate fluence determinations, as well as measurements of azimuthal distribution of thermal neutrons at the moderator surface of our standard experimental setup,

*Author for correspondence (E-mail: Westmeier@Westmeier.com).

called GAMMA-2, will be presented. Transmutation rates of ^{129}I, ^{139}La and ^{237}Np will be given for well-defined experimental conditions using protons of energies in the range from 0.53 GeV to 4.15 GeV. The main goal of these measurements is the generation of a large amount of accelerator driven transmutation results with small uncertainties that can be used as benchmark data for the necessary improvement of model calculations.

The measurement of detailed neutronics on the GAMMA-2 target, such as neutron densities and energy spectra, is of great interest for practical aspects of transmutation studies and for computerized model developers. Results for neutron density distributions measured with solid state nuclear track detectors (SSNTD) with converters on top of the target will be presented. Data are shown for two different neutron energy regimes in experiments with protons of 0.65 GeV, 1.0 GeV and 3.7 GeV impinging on the lead target.

2. Experimental setup

Our experiments were carried out with the GAMMA-2 target setup at the NUCLOTRON accelerator using protons in the energy range from 0.53 GeV to 4.15 GeV. Details of the experimental setup are given in Ref. [8]. Fig. 1 gives a schematic view of the GAMMA-2 target together with its on-line beam monitoring system. Five scintillation detectors C1 to C5 were used to monitor the beam; coincidence data from C1×C2 quantified the direct beam and C3×C4×C5 measured scattered particles from a PE target with 1 g/cm^2 thickness. Polaroid films were used for the definition of position, size and shape of the beam on target.

Transmutation and other samples on GAMMA-2 can be placed either inside the spallation target between the lead disks, or onto the surface of the lead target, *i.e.* between the lead disks and the paraffin moderator shell where they are exposed to primary spallation neutrons, or on top of the paraffin moderator where the neutron spectrum is considerably softer. Two kinds of transmutation samples have been used in these experiments:

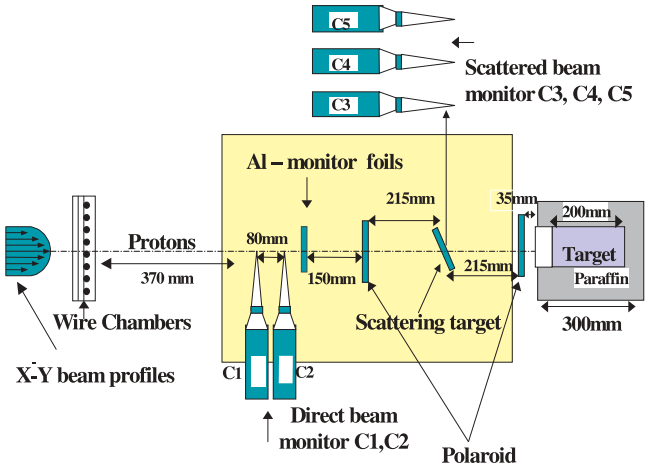

Fig. 1. Schematic view of the GAMMA-2 setup. The target is composed of 20 lead disks with 8 cm diameter and 1 cm thickness, the paraffin moderator shell has 20 cm outer diameter, 6 cm thickness and 31 cm length. The Al-monitor contains a stack of three thin aluminium foils where the center foil is used.

1. ^{129}I and ^{237}Np were taken as specimen for very long-lived and highly radiotoxic nuclides contained in nuclear waste. The selection of these nuclides was governed by availability and ease of handling.
2. ^{139}La is an inactive nuclide that has several advantages making it well suitable for transmutation studies with low-energy neutrons:

– The material is intrinsically not radioactive;
– The induced radioactivity is short lived and samples can be re-used;
– The induced radioactivity has several strong and clear γ-ray lines;
– The material normally maintains its geometrical shape;
– The material is easily weighed into the sample containers;
– The material comes in well-defined stochiometry;
– The material has a low price;
– The material is not subject to handling restrictions;
– The material is easy to dispose of.

3. Experiments on GAMMA-2

In each experiment with the GAMMA-2 target a variety of measurements is being made by many participants of an international collaboration using different transmutation samples, threshold detectors, activation samples and various kinds of solid state nuclear track detectors. Typical results from these measurements addressing different research subjects are presented in the sections below.

3.1 Measurement of the proton fluence

In order to determine proton fluences unambiguously with radiochemical methods it appeared to be useful to reconsider the cross sections of one of the commonly used radiochemical proton fluence monitor reactions, the ^{27}Al$(p,3pn)^{24}$Na reaction. Published data of cross sections for the ^{27}Al$(p,3pn)^{24}$Na reaction were re-analyzed, evaluated and least-squares fitted with an appropriate function in order to find a well defined cross section value with small uncertainty for every relevant proton energy in the range 0.5 GeV $\leq E_p \leq$ 7 GeV. Small uncertainties in the cross section values are essential as these will propagate onto the uncertainties of all experimental results. Several publications were considered in the evaluation, as given in Refs. [9] and [10] and references therein. A plot of selected cross section data is shown in Fig. 2. Data points below the proton energy of approx. 500 MeV are of no relevance to our experiments and thus a least squares fit was only made to data in the higher energy range, as indicated in the figure. The function used for the fit is an exponential polynomial of the form:

$$\sigma = \exp(a + bx + cx^2 + dx^3)\,, \qquad (1)$$

where σ is the cross section in mb, a, b, c and d are polynomial coefficiencs and x is defined as $x = \ln(z\text{-shift})$ where z is the proton energy in MeV and shift is a fit parameter. A least squares fit of the polynomial yielded the coefficients as $a = (12.122 \pm 4.322)$, $b = (-2.9337 \pm 1.4786)$, $c = (0.28684 \pm 0.18223)$, $d = (-0.00932 \pm 0.00793)$ and

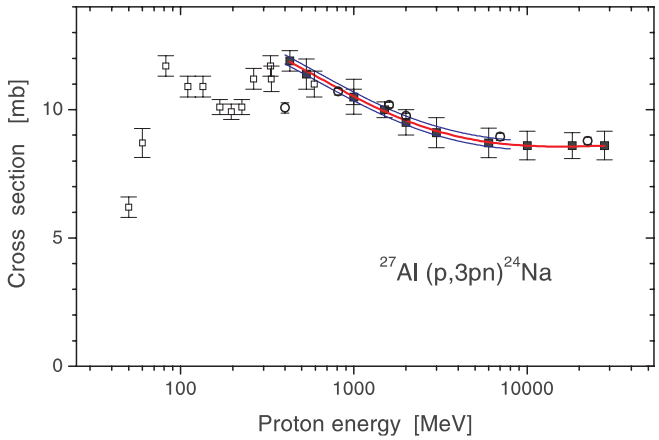

Fig. 2. Excitation function for the monitor reaction ^{27}Al$(p, 3pn)^{24}$Na. Open circles are very recent data from Ref. [16]. The central line is the fitted function and the two outer lines indicate the $\pm 1\sigma$ uncertainty range.

shift $= (-568.5 \pm 237.8)$. There is *no* physical or mathematical reason for the selection of this function but it rather fits the experimental data well. The central fit line in Fig. 2 depicts the least-squares fitted function and the two lines above and below the fitted line indicate the one standard deviation ($\pm 1\sigma$) uncertainty range of the fitted function. Cross sections values for energies of our and other relevant irradiations as calculated from the fitted function are given in Table 1. It should be noted that a very recent experimental data set from reference [16] is in excellent agreement with our fit, except one data point at 400 MeV. The reason for an apparent discrepancy for this data point is unknown but it seems worthwhile that cross sections at least in the energy range of 200 MeV $\leq E_{\mathrm{p}} \leq$ 600 MeV should be reinvestigated. Despite the fact that the selected data in Fig. 2 look very consistent and can be fitted well, there is still a lot of ambiguity in the whole set of published data. For example, the cross section at 1200 MeV proton energy is found as (data listed in the order of publication dates) 10.3 ± 0.7 mb interpolated from [9], 12.0 ± 0.9 mb [17], 10.8 ± 0.8 mb [18], 12.9 ± 0.9 mb [19], 10.4 ± 0.3 mb interpolated from [16], and 10.24 ± 0.17 mb (this work) which is a remarkably wide range of scattering of results. Without further experimental details we are unable to comment on the apparent discrepancies.

Initial information about the extracted beam intensity was obtained from operators' instrumentation in the beam-extraction channel. Aluminium activation foils were used to determine the integral proton fluence on the target. The absolute intensity of the proton beam hitting the target was determined as described elsewhere [5, 8, 10]. The Al monitor foil stack was placed approx. 60 cm upstream the Pb target in order to avoid activation from backscattered particles. In each experiment a stack of three Al foils was mounted in an aligned position with the target and perpendicular to the beam axis as shown in Fig. 1, and irradiated during the whole run. Then the center foil with a thickness of 31.0 μm (1.88×10^{20} atoms cm^{-2}) was cut into concentric rings of diameters 21 mm, 80 mm, 120 mm and 160 mm, respectively. The inner circle (21 mm) and the innermost ring (up to 80 mm) covered exactly the diameter of the lead target and thus these two foils determined the proton beam on the target. In order to optimize the geometric efficiency for the measurement of gamma-ray spectra from the Al-rings the foil samples were compressed into plastic vials of 14 mm inner diameter yielding sample thicknesses between *ca.* 1 mm and *ca.* 5 mm.

Gamma-ray spectrum analysis was carried out in a well-established conventional manner [11]. The measured activities of ^{24}Na at end-of-irradiation (EOI) were corrected for decay during the irradiation according to the known beam-burst profile, for decay between EOI and start of counting and for decay during the counting time. For each individual beam burst the extracted number of protons and the time of occurrence are known. Thus one can calculate the relative number of ^{24}Na atoms that have decayed during the irradiation and consider these in the calculation of the proton beam intensity. Table 2 gives a summary of the results of the measurement of proton

Table 1. Cross sections for the reaction ^{27}Al$(p, 3pn)^{24}$Na as used in our experiments.

Proton energy (GeV)	Cross section (mb)
0.533	11.50 ± 0.17
0.65	11.18 ± 0.17
1.00	10.51 ± 0.17
1.50	9.93 ± 0.17
2.00	9.58 ± 0.17
3.70	9.00 ± 0.18
4.15	8.92 ± 0.18
7.40	8.65 ± 0.17

Table 2. Details of beam monitoring.

Proton energy (GeV)	0.53	0.65	1.00	2.00	3.70	4.15
Proton density (10^{10} p/cm^2):						
21 mm ∅ circle	25.2 ±2.1	69.4 ±7.2	192 ±16	33.0 ±2.8	32.7 ±2.6	22.4 ±1.9
→ 80 mm ring	10.5 ±0.7	20.2 ±1.7	24.2 ± 2.0	13.8 ±1.0	37.7 ±2.5	20.6 ±1.4
→ 120 mm ring	2.10 ± 0.15	2.41 ± 0.23	1.11 ± 0.10	1.25 ± 0.14	3.15 ± 0.23	1.00 ± 0.09
→ 160 mm ring	0.37 ± 0.04	0.42 ± 0.05	0.48 ± 0.04	0.10 ± 0.02	1.55 ± 0.14	0.54 ± 0.05
Total fluence (10^{12} protons)	7.37 ± 0.36	13.6 ±0.9	18.6 ± 1.1	8.41 ± 0.48	22.1 ±1.3	11.5 ±0.7
On lead target (10^{12} protons)	5.73 ± 0.35	11.7 ±0.8	17.5 ± 2.0	7.54 ± 0.47	16.7 ±1.0	10.5 ±0.7
	=	=	=	=	=	=
Percentage (%)	77.7 ±6.0	86.1 ±6.1	94.0 ±10.6	89.6 ±5.6	75.5 ±4.3	90.4 ±7.8

fluences for the six proton irradiations presented in this paper.

3.2 Measurements using ^{139}La samples

A schematic picture of the positions of some ^{139}La samples around the GAMMA-2 target is shown in Fig. 3. The samples are placed on the surface around the paraffin shell which has a diameter of 20 cm. The inner ring in Fig. 3 indicates the Pb-target of 8 cm diameter. A duplicate La-sample (sample No. 12) was attached directly adjacent to sample No. 7 for reproducibility measurements in experiments with 0.65 GeV, 1.0 GeV and 3.7 GeV protons. Another set of samples was positioned along the beam axis on top of the paraffin moderator, where the sample spacing is 5 cm and the first sample sits over the point where the beam impinges onto the Pb target.

The reproducibility of measured values, the azimuthal asymmetry of the neutron fluence around the target and the integrated *B*-values for ^{140}La were determined experimentally using the transmutation reaction of ^{139}La. The material used for our investigations was $LaCl_3 \cdot 7H_2O$ which is a slightly hygroscopic white salt that sticks easily together and maintains its geometrical shape when handled gently. The transmutation rate in ^{139}La is determined as a $B(^{140}\mathrm{La})$-value for the nuclear activation reaction

$$^{139}\mathrm{La}(n,\gamma)^{140}\mathrm{La}\,, \tag{2}$$

where ^{140}La decays with a half-life of 40.2 hours with the emission of several strong γ-rays. The *B*-value for the reaction is defined as

$$B(^{140}\mathrm{La}) = \text{Number of atoms of } ^{140}\text{La produced in 1 gram of } ^{139}\text{La as sample material per 1 primary proton.}$$

The *B*-value for a reaction is the normalized average value of the integral of the excitation function for a nuclear reaction multiplied with the neutron spectrum at the given sample position on the setup. The definition allows intercomparison of results from different samples and (probably) for differing proton energies on a given setup, but it is critically dependent on the geometry of the experiment and the composition of its constituents. Thus, *B*-values that are measured on one specific target system cannot be numerically compared with those from other experiments using a different target. However, as we restrict ourselves to always using the identical target setup for one type of experiments, our results can be subjected even to numerical intercomparison.

3.2.1 Reproducibility of measurements with different samples

In order to test the reproducibility of measurements we exposed in three separate experiments a second ^{139}La sample (sample No. 12) directly adjacent to sample position No. 7 which is the 120° position in the measurement of the azimuthal neutron density variations (see Sect. 3.2.2). A sketch of the measurement geometry is shown in Fig. 3 where the

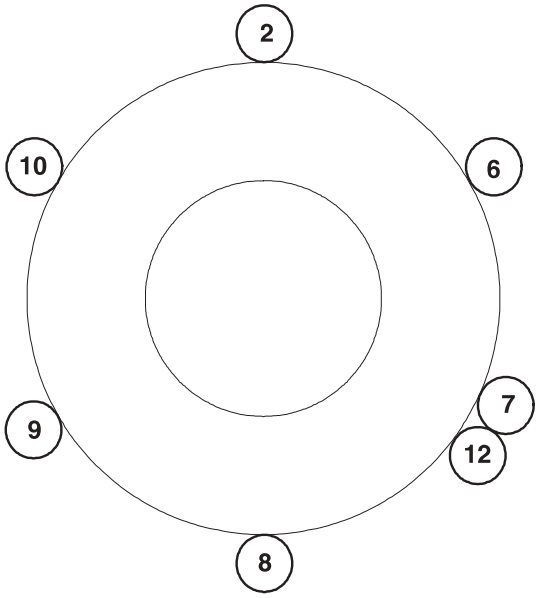

Fig. 3. Sketch of the geometrical setup for the determination of the azimuthal anisotropy and of the reproducibility of measured values.

region between the two large circles denotes the paraffin moderator shell and the small circles with numbers are the La-samples in the respective locations around the target. Next to sample position No. 7 a second La-sample was irradiated. The ratio R(reprod.) of the ^{140}La activity per gram of La in sample No.12 to the ^{140}La activity per gram of La in sample No.7 was calculated and from the resulting three ratios the weighted mean $R(\mathrm{reprod.})_{\mathrm{average}}$ was calculated as:

$$R(\mathrm{reprod.})_{\mathrm{average}} = 0.988 \pm 0.044\,. \tag{3}$$

Propagation of uncertainties was maintained throughout all calculations. The weighted average ratio of measurements of duplicate results is very close to unity and it is determined with an uncertainty of only ±4.4%. We assume that the reproducibility of results is good and that there is no need for our team to make further measurements of duplicate samples.

3.2.2 The azimuthal distribution of secondary neutrons

Five La-samples on top of the target are used to measure the integrated $B(^{140}\mathrm{La})$ (see Sect. 3.2.3) The neutron fluence on GAMMA-2 is very large around the position of the second sample and therefore this position was chosen to study the azimuthal variations of the neutron fluence. This second La-sample at 5 cm behind impact of the beam on the lead target serves simultaneously for the measurement of $B(^{140}\mathrm{La})$ along the longitudinal axis and the determination of the azimuthal variations. Six La-samples were therefore attached around the paraffin shell as schematically shown in Fig. 3. Samples were placed at azimuthal angles of 0°, 60°, 120°, 180°, 240°, and 300° where the sample on top is denoted as 0°. The anisotropy is determined through the activity at EOI of ^{140}La as counted in a calibrated position of the HPGe detector and corrected for efficiency and all decays.

In Fig. 4 the resulting azimuthal neutron density distribution from the 0.53 GeV irradiation on GAMMA-2 is shown

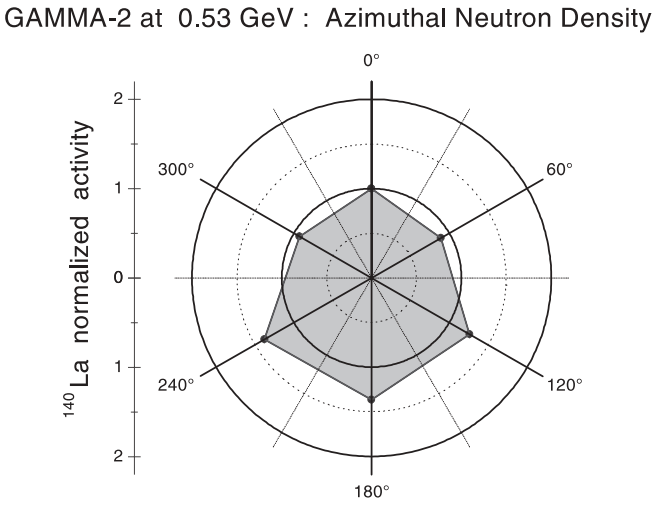

Fig. 4. Polar graph of the azimuthal neutron density distribution in the 0.53 GeV experiment. The polar coordinate is scaled as normalized activity of ^{140}La relative to the value at 0°.

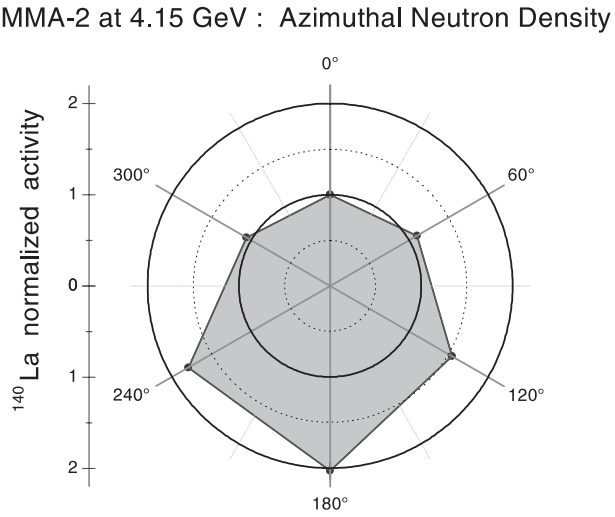

Fig. 6. Polar graph of the azimuthal neutron density distribution in the 4.15 GeV experiment.

as a polar graph, where the radial coordinate gives the normalized ^{140}La activity in one gram of La. The length of the radial coordinate of the 0° activity is denoted as unity and the other values are normalized accordingly onto a radial scale that goes from zero to two. Iso-circles have been plotted at even fractions of the counting rate of the sample at 0°. The figure shows a very symmetric neutron distribution in the upper part from 300° to 60° and a slight asymmetry from 60° to 240. The neutron density value at 120° is about 1.25 times the value at 0° and the average asymmetry with respect to 0° is calculated to be 1.136 ± 0.034. This number is the correction factor that must be applied to all *B*-values being measured at 0° on top of the GAMMA-2 setup in the 0.53 GeV experiment.

In Figs. 5 and 6 the normalized polar graphs for irradiations at two other proton energies are shown where azimuthal anisotropies are extremes. The resulting correction factors for all irradiations are summarized in Table 3. From the figures and Table 3 it is clear that in most experiments

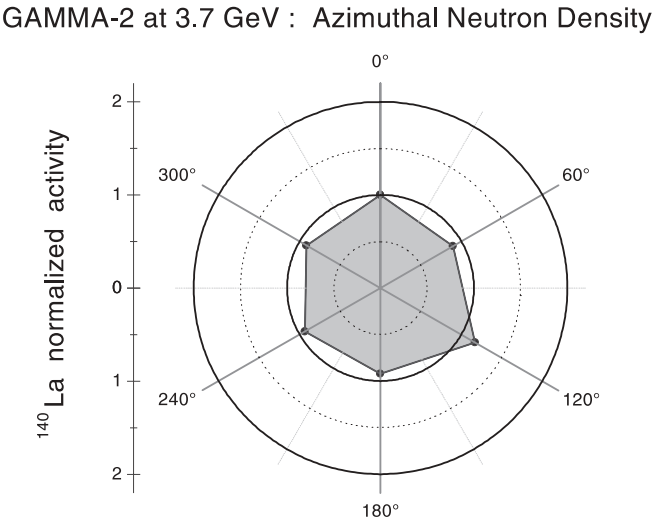

Fig. 5. Polar graph of the azimuthal neutron density distribution in the 3.7 GeV experiment.

Table 3. Azimuthal correction factors for the $B(^{140}\mathrm{La})$ calculation in proton irradiations.

Proton energy/GeV	Correction factor
0.53	1.136 ± 0.034
0.65	1.085 ± 0.059
1.00	$1,212 \pm 0.039$
2.00	1.104 ± 0.056
3.70	0.971 ± 0.036
4.15	1.419 ± 0.041

the azimuthal neutron asymmetry correction is not negligible. For proper analysis and display of experimental data it is mandatory that the asymmetry is measured and considered in each individual experiment. There is no systematic trend or dependence found for these correction factors. The azimuthal asymmetry in the neutron distributions on the surface of the paraffin can have two origins:

1) An external origin, resulting from the reflection of neutrons from surrounding material such as the irradiation table, floor and walls, *etc.*
2) An internal origin, resulting from asymmetries in beam position on entrance to the target, in beam shape and in the axial alignment of the target.

Calculations show that although an effect of neutron reflection from external material exists it can by far not explain the observed asymmetries. However, an irregular shape of the incident beam and deviation of the target axis from the incident beam direction can result in a highly asymmetric neutron distribution around the target [12].

3.2.3 Transmutation of ^{139}La

Samples containing 1 gram of lanthanum each were placed on top of the target assembly at distances of 5 cm, 10 cm, 15 cm, 20 cm, and 25 cm from the front side of the paraffin block. These locations are 0 cm, 5 cm, 10 cm, 15 cm and 20 cm from the front of the lead target, *i.e.* the first sample sits just above the location where the proton beam hits the

Table 4. $B(^{140}\mathrm{La})$-values in units of $[10^{-5}$ atoms ^{140}La in 1 g ^{139}La per 1 proton].

E_p/GeV	0 cm	5 cm	10 cm	15 cm	20 cm	B (integral)[a]
0.53	2.63 ± 0.17	3.78 ± 0.24	4.00 ± 0.26	2.46 ± 0.16	1.62 ± 0.10	102.3 ± 7.3
0.65	3.28 ± 0.22	4.51 ± 0.30	4.95 ± 0.33	3.57 ± 0.24	1.97 ± 0.13	120.6 ± 10.1
1.00	3.93 ± 0.27	5.66 ± 0.38	6.30 ± 0.43	4.73 ± 0.32	2.85 ± 0.19	176.2 ± 13.7
2.00	6.74 ± 0.47	10.45 ± 0.73	11.26 ± 0.79	9.54 ± 0.67	6.31 ± 0.45	306.9 ± 26.0
3.70	9.33 ± 0.69	12.69 ± 0.96	15.45 ± 1.15	11.94 ± 0.89	7.36 ± 0.55	347.0 ± 29.2
4.15	8.48 ± 0.56	12.62 ± 0.83	15.61 ± 1.03	13.34 ± 0.88	8.21 ± 0.58	467.8 ± 34.3

E_p is the proton energy. The distances are given in cm from the front of the Pb target;
a: B (integral) is the integrated $B(^{140}\mathrm{La})$-value as defined in the text.

Pb. B-values for each of the five samples (corrected for neutron anisotropy) were calculated in every experiment. The individual $B(^{140}\mathrm{La})$ values are listed in Table 4.

In order to compare neutron densities from various experiments we calculated the integrated $B(^{140}\mathrm{La})$ for ^{140}La on the GAMMA-2 setup by fitting the five data points with a modified (skewed) Gaussian function. The function is used because it has a suitable shape and not because of any physical significance. The least-squares fitted functions are plotted as solid lines in Fig. 7 for irradiations at 0.53 GeV, 2.0 GeV and 4.15 GeV.

The integral over a fitted function from $-\infty$ to $+\infty$ is the integrated $B(^{140}\mathrm{La})$ which will be used for comparisons later. The fitted distributions quantify findings from earlier experiments [4, 5] that the shapes of B-value distributions (*i.e.* the neutron densities over the target) are very similar over the entire proton energy range studied. The maximum of the B-values is always found at about 10 cm downstream the beginning of the lead target and the widths of the distributions are essentially the same for each energy in the $0.53\,\mathrm{GeV} \leq E_p \leq 4.15\,\mathrm{GeV}$ range.

A compilation of integrated and normalized $B(^{140}\mathrm{La})$-values on the GAMMA-2 setup is shown in Fig. 8 as a function of proton energy. The data from earlier NUCLOTRON experiments [8] are also included which were measured without an anisotropy correction. The dotted line connecting the data points just serves to guide the eye. One can see that the uncorrected datapoints fall far below the dotted line which underlines the necessity of measurement of the beam anisotropy and corresponding data correction in every experiment. Fig. 8 shows the effectiveness of the GAMMA-2 setup for transmutation of ^{139}La *via* neutron capture reactions. Thus, it also displays the effectiveness of the GAMMA-2 setup for the production of low-energy neu-

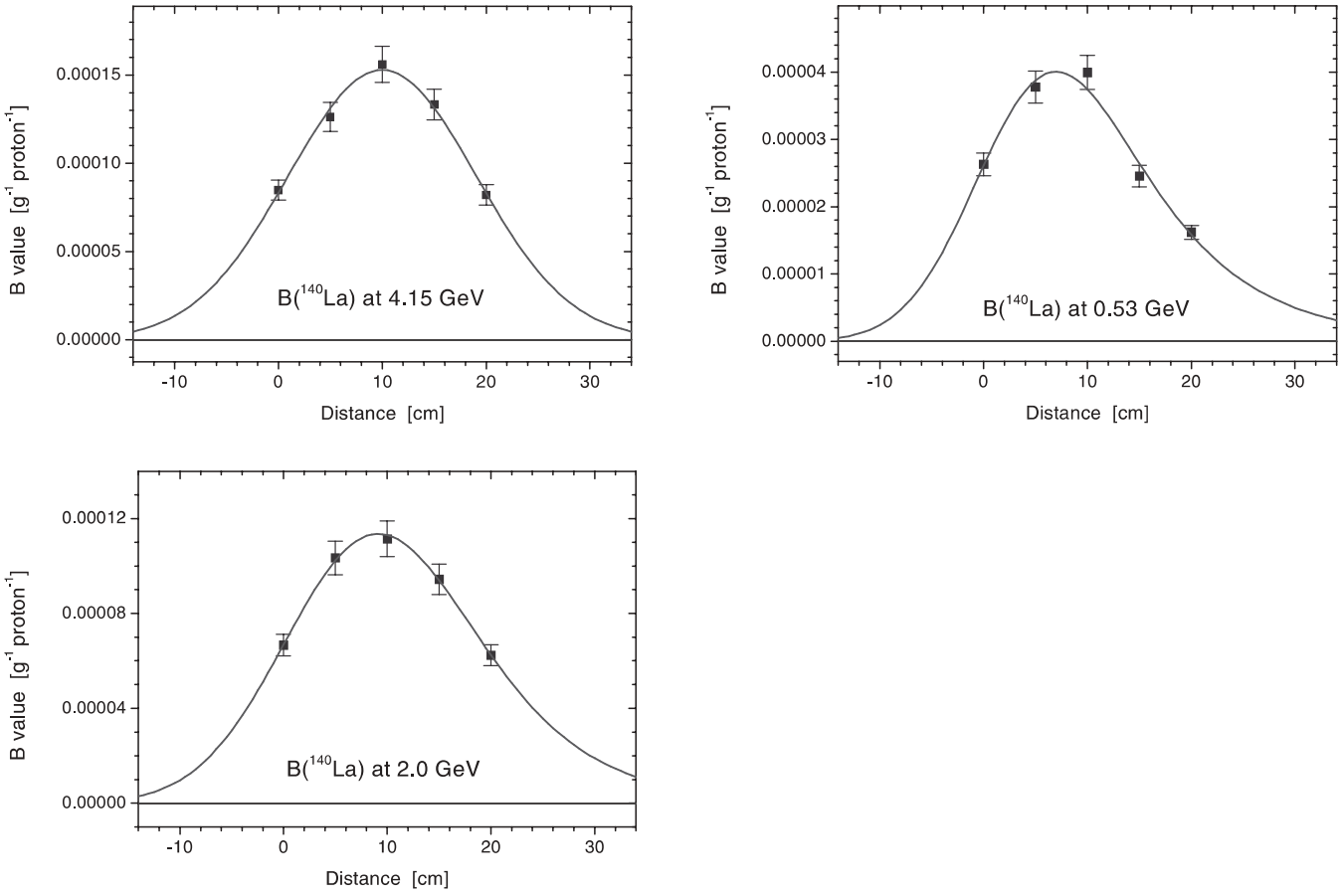

Fig. 7. B-values for ^{140}La along the top of the paraffin moderator in the irradiation with 0.53 GeV, 2.0 GeV and 4.15 GeV protons on the GAMMA-2 target. The distance $d = 0$ cm corresponds to the upsteam end of the 20 cm long Pb target, *i.e.* the point of proton impact.

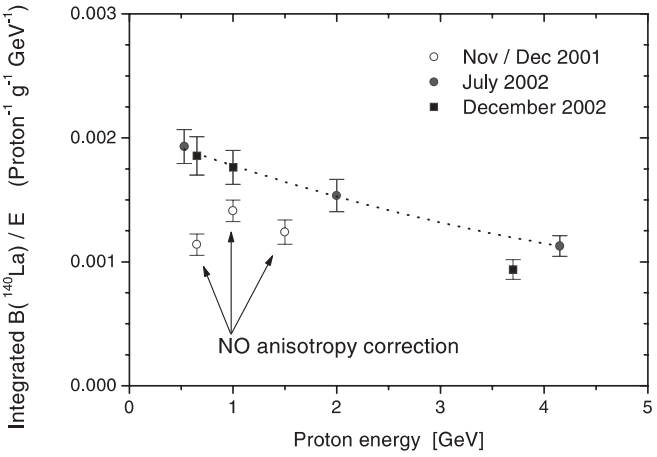

Fig. 8. Integrated and normalized B-values for ^{140}La on the GAMMA-2 setup. The dotted line serves to guide the eye.

trons. It is interesting to note that the effectiveness (also called "neutron economy" [15]) of GAMMA-2, which has only 20 cm Pb target length, for low-energy neutron production is best at low proton energies. The shape and slope of the $B(^{140}\mathrm{La})/E_\mathrm{p}$ curve are not completely consistent with calculations [13] which may well be due to the quite large diameter of the beam at low irradiation energies.

3.3 Transmutation of ^{129}I and ^{237}Np with spallation neutrons

In each experiment radioactive samples of ^{129}I and ^{237}Np were also irradiated on the surface of the paraffin moderator shell. Neutron capture (n, γ) reactions were used for transmutation and γ-rays from the decay of the product nuclei were measured:

$$^{129}\mathrm{I}(n,\gamma)^{130}\mathrm{I}\ (\beta^-, T_{1/2} = 12\ \mathrm{h}) \quad \Rightarrow {}^{130}\mathrm{Xe}\ (\mathrm{stable})\,, \qquad (4)$$

$$^{237}\mathrm{Np}(n,\gamma)^{238}\mathrm{Np}\ (\beta^-, T_{1/2} = 2.1\ \mathrm{d}) \Rightarrow \text{short-lived decay chain}\,. \qquad (5)$$

The I-samples contained between 0.3 g and 0.9 g of Iodine (85% of ^{129}I, 15% of ^{127}I) in the form of NaI salt. The material is safely encapsulated in weld-sealed aluminium containers. The containers used in the July 2002 experiment (0.53 GeV, 2.0 GeV and 4.15 GeV) had a diameter of 60 mm and side walls of 30 mm height as described in detail in Ref. [4] whereas in December 2002 we employed smaller containers of 35 mm diameter and *ca.* 15 mm height. The actual sample geometry was identical in both container types, *i.e.* the NaI samples inside each container had a diameter of 21 mm. The iodine sample was placed between the third and fourth La-sample, *i.e.* 12.5 cm from the front of the lead target, and at an angle of approx. 40 degrees from the top of the paraffin shell. After each irradiation the iodine-sample was counted several times in a calibrated position with a HPGe detector, all lines from ^{130}I were analyzed and the weighted mean activity at EOI of ^{130}I in the sample was calculated with consideration of all decays. The weighted mean activity values from various spectra were used to calculate the $B(^{130}\mathrm{I})$ value for each proton energy. The resulting normalized values are listed in Table 5 and shown in Fig. 9 (left), *i.e.* the figure shows the transmutation effectiveness for ^{129}I.

Table 5. B-values for the transmutation of ^{129}I and ^{237}Np in units of [10^{-5} atoms in one gram of sample per proton].

Proton energy E_p (GeV)	$B(^{130}\mathrm{I})$	$B(^{238}\mathrm{Np})$
0.53	11.14 ± 0.76	51.9 ± 3.6
0.65	15.36 ± 1.31	63.8 ± 5.4
1.00	16.76 ± 1.18	79.4 ± 5.7
2.00	26.55 ± 2.09	191 ± 15
3.70	40.45 ± 2.78	217 ± 15
4.15	47.47 ± 3.08	321 ± 23

The Np-samples contained between 0.99 g and 1.08 g of neptunium in the form of $^{237}NpO_2$ salt. The material is safely encapsulated in weld-sealed aluminium containers where the Np container geometries were identical to the I containers. The Np sample was placed between the third and fourth La-sample, *i.e.* 12.5 cm from the front of the lead target, and at an angle of approx. -40 degrees from the top of the paraffin shell, opposite to the iodine sample.

Sample assay and γ-ray spectrum analysis were conducted identical to the I samples. The resulting $B(^{238}\mathrm{Np})$-values are listed in Table 5 and shown in Fig. 9 (right).

Considering results from Tables 4 and 5 and Figs. 8 and 9 it is clear that the transmutation effectiveness B/E_p on the

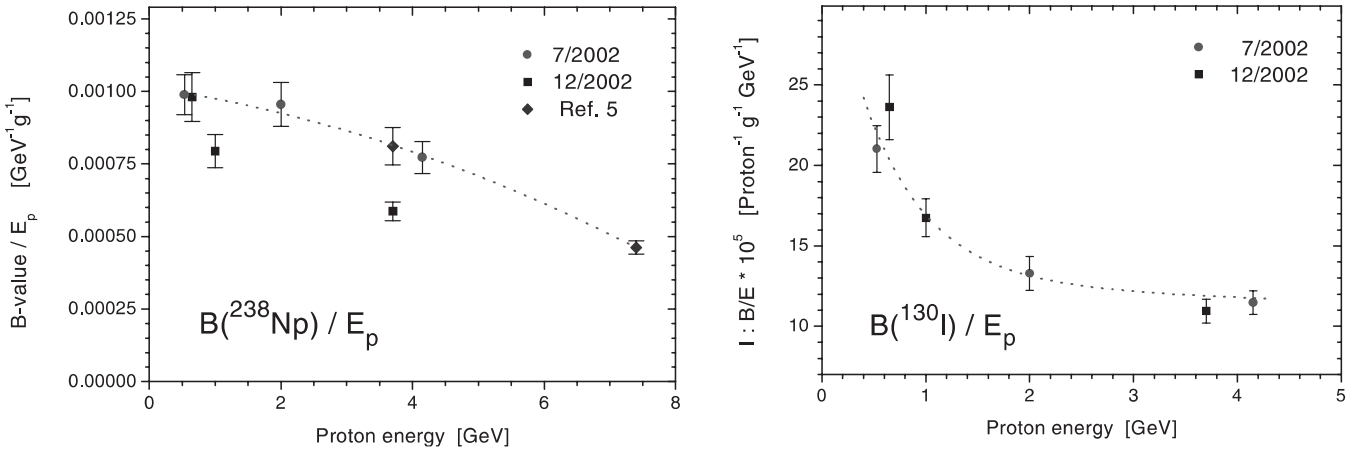

Fig. 9. Normalized $B(^{130}\mathrm{I})/E_\mathrm{p}$ and $B(^{238}\mathrm{Np})/E_\mathrm{p}$ on the surface of the GAMMA-2 setup. The dotted line serves to guide the eye.

GAMMA-2 target is always highest at low proton energy and gradually falls off with rising bombarding energy. This may be a consequence of the size of the target where the small diameter and short length do not allow the intra- and inter-nuclear cascades originating from incident protons to be completed [13].

3.4 Measurement of neutron densities on the target

Neutron density distributions were studied for slow (thermal and epithermal) as well as intermediate energy plus fast neutrons using sets of solid state nuclear track detector (SSNTD) foils that were positioned along the target on the paraffin surface. Each foil consisted of CR39 where quarter of the area was covered on both sides with 1 mm cadmium for complete absorption of thermal neutrons. Information exclusively about fast neutrons in the energy range $0.3\,\mathrm{MeV} < E_\mathrm{n} < 3\,\mathrm{MeV}$ is gathered in the Cd-covered part. Fast neutrons are detected *via* proton recoil tracks produced by (n, p) scattering in the CR39 material itself. Half of each detector was in contact with Kodak LR115-2B film that was covered with $^{6}Li_2B_4O_7$ converter material, thus allowing, in addition to fast neutrons, the detection of thermal neutrons through tracks from the $^{10}\mathrm{B}(n,\alpha)^{7}\mathrm{Li}$ and $^{6}\mathrm{Li}(n,\alpha)^{3}\mathrm{H}$ reactions. One quarter of each SSNTD detector was uncovered. The SSNTD stacks were exposed to neutrons generated by approximately 10^{11} protons on the Pb target, where the beam intensity was taken from operator's readings. Densities of fast and slow neutrons along the paraffin moderator are shown in Fig. 10 for proton energies of 0.65 GeV, 1.0 GeV and 3.7 GeV. Uncertainties of track densities were estimated as the standard deviation of the scanned track densities of 25 fields counted in each detector. The conversion of the track density into the neutron density was made by use of an appropriate calibration [14]. Total uncertainties were calculated considering error propagation for each conversion factor in every energy range.

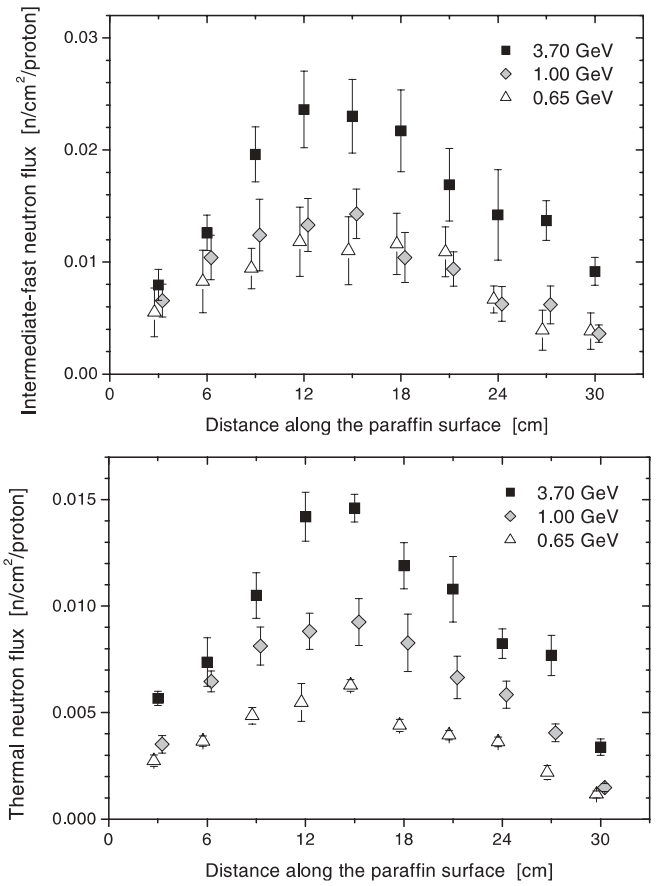

Fig. 10. Neutron densities per incoming proton of fast (top) and slow (bottom) neutrons along the paraffin surface.

All neutron distributions along the paraffin surface have very similar widths and exhibit a maximum around the middle of the target length, in good agreement with low-energy neutron density measurements *via* $B(^{140}\mathrm{La})$ distributions. The position of the maximum may be related to the interaction length, which for this energy range of primary protons is about 18 cm [15].

4. Conclusions

The new modern accelerator NUCLOTRON at the Veksler and Baldin Laboratory of High Energies in the Joint Institute for Nuclear Research in Dubna has proven to be a very suitable tool for detailed studies of proton induced transmutation in accelerator driven systems.

Relative transmutation yields defined as *B*-values were measured for ^{139}La and for the highly radiotoxic waste nuclides ^{129}I and ^{237}Np in the proton energy range from 0.5 GeV to 4.15 GeV. Shapes of *B*-value distributions for ^{140}La are in good agreement with neutron density measurements using solid state nuclear track detectors. The transmutation effectiveness in our target, *i.e.* the energy-weighted transmutation cross section, is measured largest at low proton energy and then decreases with rising energy. This may favour the use of proton beam energies that are lower than it has been assumed in other design studies. Operating at lower energy would of course be commercially attractive.

Fundamental experiments on one GAMMA-2 target setup have been completed in that a large set of high quality experimental data with small uncertainties have been generated which serve as benchmark data and can be used for modelling purposes. However, additional measurements using the same simple, symmetric GAMMA-2 setup but with a considerably longer lead target core will be made.

The reproducibility of our measured values is good, *i.e.* our data are considered to be reliable even when we have measured a data point only once.

It seems to be essential that the azimuthal asymmetry of the neutron distribution is measured in every experiment and corresponding corrections are applied to the data.

Acknowledgment. We are grateful to the "Institute of Physics and Power Engineering" in Obninsk, Russia, for producing excellent samples of radioactive nuclides ^{129}I and ^{237}Np.

Special gratitude is due to Professor A. D. Kovalenko and his NUCLOTRON crew who supplied stable high intensity beams even under difficult operating conditions.

We thank Professor A. I. Malakhov and the staff of LHE for the generous support of our work. They made it possible that we could irradiate even outside of scheduled times and thus more experiments were completed and data measured than initially anticipated.

Results described in the present work were obtained with the financial support of the FZ Jülich and of the JINR Directorate who provided the operation of the accelerator and other installations of the Institute.

References

1. Kovalenko, A. D.: Proc. EPAC-94. London, June 1994, V. 1, p. 161 (1995); Agapov, N. N., Kovalenko, A. D., Malakhov, A. I.: NUCLOTRON: new results and plans for development. Atomnai Energia **93**, 479 (2002) (in Russian), http://sunhe1.jinr.ru/page/nucl/nuclotron.html.
2. Tolstov, K. D.: Some aspects of accelerator breeding. JINR-preprint 18-89-778, Dubna (1989).
3. Bowman, C. D., Arthur, E. D., Lisowski, P. W., Lawrence, G. P., Jensen, R. J., Anderson, J. L., Blind, B., Cappiello, M., Davidson, J. W., England, T. R., Engel, L. N., Haight, R. C., Hughes III, H. G., Ireland, J. R., Krakowski, R. A., Labauve, R. J., Letellier, B. C., Perry, R. T., Russel, G. J., Staudhammer, K. P., Versamis, G., Wilson, W. B.: Nuclear energy generation and waste transmutation using an accelerator-driven intense thermal neutron source. Nucl. Instrum. Methods A **320**, 336 (1992); Carminata, F., Klapisch, R., Revol, J. P., Roche, Ch., Rubio, J. A., Rubbia, C.: An energy amplifier for cleaner and inexhaustible nuclear energy production driven by a particle beam accelerator. CERN, Geneva, print CERN/AT/93-47 (ET), November 1 (1993).
4. Wan, J.-S., Schmidt, Th., Langrock, E.-J., Vater, P., Brandt, R., Adam, J., Bradnova, V., Bamblevski, V. P., Geloviani, L., Gridnev, T. D., Kalinnikov, V. G., Krivopustov, M. I., Kulakov, B. A., Sosnin, A. N., Perelygin, V. P., Pronskikh, V. S., Stegailov, V. I., Tsoupko-Sitnikov, V. M., Modolo, G., Odoj, R., Phlippen, P.-W., Zamani-Valassiadou, M., Adloff, J. C., Debeauvais, M., Hashemi-Nezhad, S. R., Guo, S.-L., Li, L., Wang, Y.-L., Dwivedi, K. K., Zhuk, I. V., Boulyga, S. F., Lomonossova, E. M., Kievitskaja, A. F., Rakhno, I. L., Chigrinov, S. E., Wilson, W. B.: Transmutation of ^{129}I and ^{237}Np using spallation neutrons produced by 1.5, 3.7 and 7.4 GeV protons. Nucl. Instrum. Methods, Phys. Res. A **463**, 634 (2001); Krivopustov, M. I., Adam, J., Bradnova, V., Brandt, R., Butsev, V. S., Golubev, P. I., Kalinnikov, V. G., Karachuk, J., Kulakov, B. A., Langrock, E.-J., Modolo, G., Ochs, M., Odoj, R., Premyshev, A. N., Pronskich, V. S., Schmidt, Th., Stegailov, V. I., Wan, J. S., Zupko-Sitnikov, V. M.: First experiments on transmutation studies of ^{129}I and ^{237}Np using relativistic protons of 3.7 GeV. J. Radioanal. Nucl. Chem. **222**(1–2), 267 (1997).
5. Adam, J., Adloff, J. C., Balabekyan, A., Bamblevski, V. P., Barabanov, M. Y., Brandt, R., Bradnova, V., Chaloun, P., Debeauvais, M., Dwivedi, K. K., Guo, S.-L., Hashemi-Nezhad, S. R., Hella, K. M., Kalinnikov, V. G., Kievets, M. K., Krivopustov, M. I., Kulakov, B. A., Langrock, E.-J., Li Li, Lomonosova, E. M., Modolo, G., Odoj, R., Perelygin, V. P., Pronskikh, V. S., Solnyshkin, A. A., Sosnin, A. N., Stegialov, V. I., Tsoupko-Sitnikov, V. M., Vater, P., Wan, J.-S., Westmeier, W., Zamani-Valasiadou, M., Zhuk, I. V.: Transmutation of ^{239}Pu and other nuclides using spallation neutrons produced by relativistic protons reacting with massive U- and Pb-targets. Radiochim. Acta **90**, 431 (2002).
6. Andriamonje, S., Angelopoulos, A., Apostolakis, A., Attale, F., Brillard, L., Buono, S., Calero, J., Carminati, F., Casagrande, F., Cennini, P., Charalambous, S., DelMoral, R., Eleftheriadis, C., Gallego, E., Galvez, J., Garcia-Tabares, L., Geles, C., Goulas, I., Giorni, A., Gonzales, E., Hussonnois, M., Jaren, J., Klapisch, R., Kokkas, P., Lemeilleur, F., Lindecker, G., Liolios, A., Loiseaux, J. M., Lopez, C., Lorente, A., Macri, M., Martinez-Val, J. M., Nifenecker, H., Oropesa, J., Pavlopoulos, P., Pinston, J. A., Revol, J.-P., Roche, C., Rubbia, C., Rubio, J. A., Sakelariou, K., Sakelliou, L., Saldaña, F., Schussler, F., Tamarit, J., Trubert, D., Viano, J. B., Vieira, S., Vlachos, S., Xuan Li, Zarris, G.: Experimental determination of the energy generated in nuclear cascades by a high energy beam. Phys. Lett. B **348**, 697 (1995).
7. Abánades, A., Aleixandre, J., Andriamonje, S., Angelopoulos, A., Apostolakis, A., Arnould, H., Belle, E., Bompas, C. A., Brozzi, D., Bueno, J., Buono, S., Carminati, F., Casagrande, F., Cennini, P., Collar, J. I., Cerro, E., DelMoral, R., Díez, S., Dumps, L., Eleftheriadis, C., Embid, M., Fernández, R., Gálvez, J., García, J., Gelès, C., Giorni, A., González, E., González, O., Goulas, I., Heuer, D., Hussonnois, M., Kadi, Y., Karaiskos, P., Kitis, G., Klapisch, R., Kokkas, P., Lacoste, V., Le Naour, C., López, C., Loiseaux, J. M., Martínez-Val, J. M., Méplan, O., Nifenecker, H., Oropesa, J., Papadopoulos, I., Pavlopoulos, P., Pérez-Enciso, E., Pérez-Navarro, A., Perlado, M., Placci, A., Poza, M., Revol, J.-P., Rubbia, C., Rubio, J. A., Sakelliou, L., Saldaña, F., Savvidis, E., Schussler, F., Sirvent, C., Tamarit, J., Trubert, D., Tzima, A., Viano, J. B., Vieira, S., Vlachoudis, V., Zioutas, K.: Results from the TARC experiment: spallation neutron phenomenology in lead and neutron-driven nuclear transmutation by adiabatic resonance crossing. Nucl. Instrum. Methods, Phys. Res. A **478**, 577 (2002).
8. Adam, J., Barabanov, M. Yu., Bradnova, V., Brandt, R., Chaloun, P., Hella, Kh.. M., Hashemi-Nezhad, S. R., Kalinnikov, V. G., Krasnov, V. A., Krivopustov, M. I., Kulakov, B. A., Odoj, R., Pronskikh, V. S., Robotham, H., Solnyshkin, A. A., Sosnin, A. N., Stegailov, V. I., Tsoupko-Sitnikov, V. M., Westmeier, W.: First nuclear activation experiments using the new accelerator NUCLOTRON in Dubna. Kerntechnik **68**(5–6), 214 (2003); JINR preprint E1-2002-233, Dubna (2002).
9. Cumming, J. B.: Ann. Rev. Nucl. Sci. **13**, 261 (1963); Münzel, H., Klewe-Nebenius, H., Lange, J., Pfennig, G., Hemberle, K., Neumann, B.: Karlsruhe Charged Particle Reaction Data Compilation. Physics Daten/Physics Data 15-5, ISSN 0344-8401 (1982).
10. Wan, J.-S., Ochs, M., Vater, P., Song, X. P., Langrock, E.-J., Brandt, R., Adam, J., Bamblevski, V. P., Kulakov, B. A., Krivopustov, M. I., Sosnin, A. N., Modolo, G., Odoj, R.: Monitor reactions in Al-foils for high energy proton beams bombarding a thick target. Nucl. Instrum. Methods, Phys. Res. B **155**, 110 (1999).
11. Westmeier, W.: Benutzerhandbuch des Gamma Spektrenanalyse Programmes GAMMAW, Version 10.32. Gesellschaft für Kernspektrometrie mbH, D-35085 Ebsdorfergrund, Germany (2002).
12. Hashemi-Nezhad, S. R., *et al.*: unpublished (2003).
13. Hashemi-Nezhad, S. R., Brandt, R., Westmeier, W., Bamblevski, V. P., Krivopustov, M. I., Kulakov, B. A., Sosnin, A. N., Wan, J.-S., Odoj, R.: Monte Carlo analysis of accelerator driven systems: Studies on spallation neutron yield and energy gain. Kerntechnik **66**, 47 (2001).
14. Stoulos, S., Fragopoulou, M., Manolopoulou, M., Sosnin, A., Krivopustov, M. I., Westmeier, W., Brandt, R., Debeauvais M., Zamani, M.: Neutron measurements by passive methods in the Dubna transmutation assemblies. Nucl. Instrum. Methods, Phys. Res. A **519**, 651 (2003).
15. Letourneau, A., Galin, J., Goldenbaum, F., Lott, B., Péghaire, A., Enke, M., Hilscher, D., Jahnke, U., Nünighoff, K., Filges, D., Neef, R. D., Paul, N., Schaal, H., Sterzenbach, G., Tietze, A.: Neutron production in bombardments of thin and thick W, Hg, Pb targets by 0.4, 0.8, 1.2, 1.8 and 2.5 GeV protons. Nucl. Instrum. Methods, Phys. Res. B **170**, 299 (2000).
16. Morgan, G. L., Alrick, K. R., Saunders, A., Cverna, F. C., King, N. S. P., Merill, F. E., Waters, L. S., Hanson, A. L., Greene, G. A., Liljestrand, R. P., Thompson, R. T., Henry, E. A.: Total cross sections for the production of ^{22}Na und ^{24}Na in proton-induced reactions on ^{27}Al from 0.40 to 22.4 GeV. Nucl. Instrum. Methods, Phys. Res. B **211**, 297 (2003).
17. Dittrich, B., Herpers, U., Lüpke, M., Michel, R., Signer, P., Wieler, R., Hofmann, H. J., Wölfli, W.: Progress Report on Nuclear Data Research in the Federal Republic of Germany for the Period April 1, 1989 to March 31, 1990. NEANDC(E)-312-U Vol. V INDC(Ger)-35/LN+Special (1990) p. 45.
18. Michel, R., Gloris, M., Lange, H.-J., Leya, I., Lüpke, M., Herpers, U., Dittrich-Hannen, B., Rösel, R., Schiekel, Th., Filges, D., Dragovitsch, P., Suter, M., Hofmann, H.-J., Wölfli, W., Kubik, P., Baur H., Wieler, R.: Nuclide production by proton-induced reactions on elements ($6 \leq Z \leq 29$) in the energy range from 800 to 2600 MeV. Nucl. Instrum. Methods, Phys. Res. B **103**, 183 (1995).
19. Titarenko, Yu. E., Shvedov, O. V., Batyaev, V. F., Karpikhin, E. I., Zhivun, V. M., Koldobsky, A. B., Mulambetov, R. D., Kvasova, S. V., Sosnin, A. N., Mashnik, S. G., Prael, R. E., Sierk, A. J., Gabriel, T. A., Saito, M., Yasuda, H.: Cross sections for nuclide production in 1 GeV proton-irradiated ^{208}Pb. Phys. Rev. C **65**, 064 610 (2002).